ECO-FRIENDLY BIONANOCOMPOSITE BASED ON BIOSYNTHESIZED POLY(3-HYDROXYBUTYRATE-CO-3-HYDROXYVALERATE) REINFORCED WITH Ni-CuO NANOPARTICLES FOR REMOVAL OF BRILLIANT GREEN

MOHAMMAD I. IBRAHIM,[*] KHALID A. ALAMRY,[*] DIYA ALSAFADI,[**] RAED ALTHOMALI,[***] MOHAMED A. ABDEL-FADEEL,[*] MOHD RAFATULLAH[****] and MAHMOUD A. HUSSEIN[*,*****]

[*]*Chemistry Department, Faculty of Science, King Abdulaziz University, Jeddah 21589, B.O. Box 80203 Saudi Arabia*
[**]*Biocatalysis and Biosynthesis Research Unit, Advanced Research Center, Royal Scientific Society, Amman 11941, Jordan*
[***]*Department of Chemistry, College of Art and Science, Prince Sattam bin Abdulaziz University, Wadi Al-Dawasir 11991, Saudi Arabia*
[****]*Division of Environmental Technology, School of Industrial Technology, Universiti Sains Malaysia, 11800 Penang, Malaysia*
[*****]*Chemistry Department, Faculty of Science, Assiut University, Assiut 71516, Egypt*
✉ *Corresponding authors: K.A. Alamry, kaalamri@kau.edu.sa*
M.A. Hussein, mahussein74@yahoo.com, maabdo@kau.edu.sa

Received January 11, 2024

Ni-doped Copper oxide (Ni-CuO) nanoparticles have been synthesized from Arabic Gum. Poly(3-hydroxybutyrate-co-3-hydroxyvalerate) (PHBV) polyester was biosynthesized by the microorganism *Haloferax mediterranei* utilizing date waste as carbon source. The produced Ni-doped copper oxide (Ni-CuO) nanoparticles have been incorporated with different percentages into the PHBV matrix. The produced bionanocomposites were achieved with different percentages of the nanoparticles: 1%, 3%, 5% and 10%, and were referred to as PHBV/Ni-CuO$_{(1,3,5,10\%)}$. FTIR, TGA, XRD, SEM and EDX techniques have been used to study and characterize the synthesized bionanocoposites. In addition, the prepared nanocomposites were studied for their efficiency as solid phase adsorbents for Brilliant Green (B.G.) dye from water resources under different conditions. The prepared nanocomposites were found to be very efficient and promising solid phase adsorbent materials to treat water samples for the purpose of dye removal. The percentage of the removed dye increased from 45.6% to 97.7% as the PHBV/Ni-CuO$_{(10\%)}$ nanocomposite amount increased from 10 mg to 70 mg per 25 mL of water sample. The dye removal percentage reached an equilibrium in 90 min. Natural water samples from three different sources have been tested against the Ni-CuO/PHBV$_{(3\%)}$ nanocomposite as solid adsorbent for the B.G. removal, and the results showed >90% dye removal in all cases under the optimum experimental conditions.

Keywords: poly(hydroxybutyrate-co-valerate), bionanocomposite, Ni-CuO, dye removal, Brilliant Green

INTRODUCTION

Poly(3-hydroxybutyrate-*co*-3-hydroxyvalerate) (PHBV) is a polyester copolymer that has good mechanical properties and lower melting point when compared to poly(3-hydroxybutyrate) (PHB).[1,2] It is also easier for processing as it has lower glass transition and melting temperatures.[3,4] In addition, it has lower crystallinity and hence it is less brittle. Also, it has higher biodegradability with increasing valerate percentage.[5,6] The PHBV has many favorable features, like low cytotoxicity, biological origin, biodegradability, thermoplasticity, piezoelectric-city, it is biocompatible with various types of cells, soluble in chlorinated solvents, has chemical inactivity, ultraviolet radiation resistivity, excellent oxygen barrier properties, but still it is a relatively brittle polymer, with low impact resistance and poor thermal stability.[7-10]

PHBV has been investigated for many applications in biomedical fields, of which bone scaffolds, drug delivery systems and tissue engineering were the main ones.[11]

Despite the limitations in PHBV properties and process costs,[12] numerous published research works have reported the synthesis of biocomposites using different types of filler materials to enhanced its properties and direct it to be utilized in different applications.[13] Applications were focused on tissue engineering, drug delivery and packaging, among others. Fillers of bio-origin were mostly used in order to produce totally biodegradable composites. PHBV biocomposites and their applications have been reviewed.[13-16] Copper oxide (CuO) nanoparticles within melt mixed PHBV nanocomposites were synthesized. The oxygen barrier properties were enhanced with 0.05 wt% CuO, and the water vapor permeability has increased as well. In addition, considerable virucidal and bactericidal properties were reported against the borne pathogens *Listeria monocytogenes*, *Salmonella enterica* and *Murine norovirus* when lower copper oxide loading amounts were loaded.[17]

In another study, the addition of CuO nanoparticles to PHBV has resulted in nanocomposites with higher modulus of elasticity and better mechanical properties at elevated temperatures; they have also supported the growth of fibroblasts over time.[18] Also, poly(3-hydroxybutyrate) (PHB) was blended with polyamine and investigated as a carrier for the drug norfloxacin. Different amounts of NiO nanoparticles were added. It was found that the release of the drug was slower from the nanocomposite compared to NiO, PHB/polyamine blend and PHB, and it was found that the higher the ratio of NiO content the slower the rate of the release was. In addition, it was reported that the inclusion of NiO within the PHB/polyamine matrix had a higher efficacy against *Pseudomonas aeruginosa* and *Streptococcus pyogenes* than the free drug norfloxacin.[19]

The release of industrial effluents and the substantial use of pesticides and fertilizers in agricultural fields result in pollution or contamination of natural water resources.[20,21] The treatment of industrial effluents is essential for their reutilization for industry or other activities after the removal of hazardous chemicals.[22–24] Dyes are an integral part of the pollutants in industrial effluents.[25–27] Food, textile, pharmaceuticals, printing, paper, leather and cosmetic industries are the main industries discharging dyes into the aquatic environment,[28–30] in which, the textile industry is the most important contributor. As a considerable number of hazardous chemicals exist in the dye effluents, their serious effects on human health and their impact on the aquatic life and environment, dye treatment has received remarkable attention.[31–33] Toxic amines, which are released from dye decomposition, can have serious impacts on the health of both humans and animals. In addition, the photosynthesis process is also affected by the dye color, as these could work as photo shields that prevent light penetration.[34–37] These aforementioned consequences of pollution caused by dyes raise the need to develop new materials for the purpose of removing these chemicals either by chemical or physical processes.

Adsorption onto solid phase materials is one of the very promising fields for the treatment of environmental and industrial effluents, of which nanomaterials with their nanoparticle sizes, large surface areas with abundant reactive sites and nanostructures are of huge interest, as they are considered efficient adsorbents for the treatment of wastewater, removal of textile dyes for wastewater remediation.[38-43] In this study, bionanocomposites comprising PHBV and Ni-CuO nanoparticles have been synthesized, characterized and investigated. The Ni-CuO nanoparticles were synthesized from Arabic Gum. In addition, the PHBV has been biosynthesized utilizing date waste as carbon source. The prepared nanocomposites were studied for their efficiency as solid phase adsorbent for Brilliant Green (B.G.) dye from natural waters under different conditions.

EXPERIMENTAL

Materials

Haloferax mediterranei was obtained from Leibniz Institute DSMZ (Germany), as lyophilized sample of strain DSM1411. *H. mediterranei* was initially grown in nutrient-rich AS-168 medium. Nickel sulfate hexahydrate and copper sulfate pentahydrate were purchased from Sigma Aldrich (99%, Germany). Sodium hydroxide was purchased from PDH (99%, UK). Chloroform was also purchased from Sigma Aldrich (99%, Germany). Gum Arabic was purchased from a Saudi local market. All solvents and reagents were used as purchased, without any additional purification.

Biosynthesis of PHBV polyester

PHBV has been biosynthesized by the halophilic archaeon *Haloferax mediterranei* from date palm tree waste biomass as feedstock, and with relatively high 3-hydroxyvalerate (3 HV) content of around 18.0 mol%. The produced PHBV is of narrow polydispersity (PDI = 1.5), high molecular weight (746.0 kDa) and a melting point of 148.1 °C, the details of the biosynthesis were previously reported. The complete details of synthesis and characterization have been previously described in published research.[44]

Synthesis of Ni-doped CuO nanoparticles using Gum Arabic (GA)

To synthesize Ni-CuO nanoparticles, 50 mL of $NiSO_4.6H_2O$ (0.01 M) solution was poured to 50 mL of $CuSO_4.5\ H_2O$ (0.1 M) and the resultant solution was stirred for 30 min. Then, 40 mL of Gum Arabic (GA) solution (1% (w/v)) was also added with additional 30 min stirring. Using 1 M NaOH solution drops, the pH of the solution was adjusted to pH ~10 and stirring was extended for another 90 min at room temperature. The resultant colloidal solution was left for 24 h at room temperature and then was centrifuged. The resultant product was then washed with ethanol and distilled water and then left to dry at 60 °C. The dry product was then calcined at 450 °C for 60 min in a muffle furnace.

Synthesis of PHBV/Ni-CuO biocomposites

Different amounts of Ni-CuO (0.007 g, 0.021 g, 0.035 g, 0.07 g) nanoparticles were weighed and added separately to glass tubes with 5 mL $CHCl_3$ in each, and the suspensions were sonicated for 15 minutes. In four 50 mL beakers, 0.7 g of PHBV polymer was dissolved in 18 mL $CHCl_3$ in each of the four beakers with stirring for 30 minutes. The nanoparticle suspensions in $CHCl_3$ were poured separately into the four 50 mL beakers containing the PHBV polymer dissolved in $CHCl_3$, and the resultant four mixtures were stirred for 5 minutes. Then, the four formed suspensions were poured separately into watch glasses, covered with glass covers and left to dry. The formed bionanocomposites (1%, 3%, 5% and 10%) were then taken and characterized.

Analysis methods

Scanning electron microscopy (SEM) analysis

Images were taken after coating the samples with a 10 nm gold layer by sputter coating and the SEM system used was JCM-7000 NeoScope™ Benchtop SEM/Jeol.

X-ray diffraction

The XRD patterns of the composites were recorded using a Panalytica X'pert PRO MPD X-Ray Diffractometer, with Cu-Kα radiation source (λ = 0.15418 nm), maximum X-ray power of 45 kV and 40 mA.

Thermogravimetric analysis (TGA)

High resolution dynamic thermogravimetric analyses (TGA) were done under a continuous flow of nitrogen on a Hi-Res TGA Q500 (TA Instruments) thermogravimetric analyzer, at a heating rate of 5 °C per minute.

Fourier transform infrared (FT-IR) spectroscopy

FT-IR spectra (4000-600 cm^{-1}) were performed in the solid state on a Thermo Fisher Scientific Nicolet 700 FT-IR Spectrometer (voltage: 100/240 V, beam splitter: KBr/Ge mid-infrared optimized).

Dye removal investigation

Reagents and materials

All solvents and chemicals used were of analytical grade with no further purification. A stock solution of Brilliant Green (B.G.) dye (100 μg mL^{-1}) was prepared (Aldrich Chemical Co Ltd., Milwaukee, WC., USA). Serial diluted solutions of (5–25 μg mL^{-1}) were also prepared using the stock solution. A series of Bitton-Robinson (BR) buffer of pH 2-11, NaOH and/or HCl (0.1 mol L^{-1}) were used as extraction media in dye sorption process by the nanocomposite.

Apparatus for dye removal assessment

All UV-Vis spectrophotometric analyses were performed on a UV–visible (190–1100 nm) spectrophotometer, with 10 mm (path width) quartz cell (Perkin-Elmer, model Lambda 25, USA). An Orion pH meter (model EA 940) was used for pH measurements. A micropipette (Volac) was used for the preparation of dye standards. The used digital balance was from BT technology model ADP 110L (max. capacity: 110 g, readability: 0.001 g). Deionized water was produced using a water purification system model Milli-Q Plus (Millipore, Bedford, MA, USA).

Dye removal procedure

Samples of 0.03 ± 0.002 g of solid phase nanocomposite were mixed with an aqueous solution (25 mL) that contained B.G. dye (5 mg L^{-1}) at pH = 6. The mixtures were shaken for 90 min on a mechanical shaker. The amount of remaining dye in the aqueous solution was then measured spectrophotometrically.[45] The amount of dye removed by the solid phase nanocomposite was calculated through the difference of absorbance between the dye aqueous solution before (A_b) and after adding the solid phase adsorbent and shaking (A_f). The amount of dye retained at equilibrium (q_e) per unit mass of solid phase (mol g^{-1}), the sorption percentage (% E) and the distribution coefficient (K_d) of sorbed analyte onto the nanocomposite were calculated. The reported % E and K_d were calculated as the average of three measurements with precision close to ±2%. Also, the effects of temperature, solution ionic strength, amount of solid phase and shaking time and on the retention of

dye by the nanocomposite sorbent were investigated.

Environmental sample collection for dye removal application

Samples of Red Sea water, tap water and wastewater were used to assess the efficiency of the nanocomposite sorbents for the extraction of dyes. Red Sea water was obtained from the Red Sea coast at Jeddah City, KSA, tap water was obtained from the chemistry department laboratories at King Abdul Aziz University, Jeddah City, KSA, and the wastewater sample was collected from the treatment plant at King Abdulaziz University, Jeddah City, KSA. After filtering the samples through a 0.45 µm membrane filter, they were kept in Teflon bottles in the dark at 5 °C. 100 mL samples were adjusted to pH = 6, then Brilliant Green dye was added to obtain a concentration of 5 mg L^{-1}, then the solid phase sorbent was weighed and added. The amounts of removed dye were calculated as described before.

Methodology used for adsorption isotherm, kinetic and thermodynamic characterization

The Weber-Morris model was utilized in the study to conduct additional research on the sorption process (Eq. 1). The calculation of the half-life time ($t_{1/2}$) of dye sorption from the aqueous solutions onto the solid sorbents Ni-CuO/PHBV$_{(3\%)}$ provided evidence in support of the conclusion drawn from the effect of the shaking time. The $t_{1/2}$ values determined from the log C/Co versus time graphs for the sorption of B.G. dye onto Ni-CuO/PHBV (3%). $t_{1/2}$ was determined to be 1.6 ± 0.05 min:

$$q_t = R_d(t)^{1/2} \quad (1)$$

where qt is the concentration of sorbed B.G. dye at time t and Rd is the intraparticle transport rate constant.

The Freundlich equation was also used to generate a fractional power function kinetic model, which was used to explain the adsorption process. The following equation (Eq. 2) can be used to establish the fractional power function kinetic model, which was modified from the Freundlich equation. The formula used was:

$$\ln q_t = \ln a + b \ln t \quad (2)$$

where qt (mg/g) represents the quantity of B.G. dye species that has been adsorbed per mass of Ni-CuO/PHBV$_{(3\%)}$ at any given time t, and a and b are coefficients, with b < 1.

One of the most frequently used equations for describing the rate of adsorption in liquid-phase systems is the Lagergren equation. The Lagergren equation (Eq. 3) was applied to the change of B.G. dye species' sorption from aqueous media onto the Ni-CuO/PHBV$_{(3\%)}$ solid phase:

$$\log (q_e - q_t) = \log q_e - k_{lager}\, t / 2.303 \quad (3)$$

where K_{Lager} is the first order overall rate constant for the retention process, t is the time, and q_e is the amount of dye species sorbed at equilibrium per unit mass of sorbent.

Assuming that: (i) the adsorbate concentration is constant through time, and (ii) the total number of binding sites depends on the amount of adsorbate adsorbed at equilibrium, the pseudo-second order equation was further clarified. The following equation (Eq. 4) describes the pseudo-second order rate in linear form:

$$\frac{t}{qt} = \frac{1}{h} + \left(\frac{1}{qe}\right) t \quad (4)$$

where q_e and qt are the amounts adsorbed per unit mass at equilibrium and at any time, and $h = k_2 q_e^2$ can be thought of as the initial sorption rate.

The Elovich model (Eq. 5) is a common method of expressing the rate equation based on adsorption capacity. This method works well for situations where the adsorbing surface is diverse and is mostly applicable to kinetics. The following equation can be utilized to represent this model:

$$\mathbf{qt} = \boldsymbol{\beta} \ln(\boldsymbol{\alpha\beta}) + \boldsymbol{\beta} \ln \boldsymbol{t} \quad (5)$$

where α (g.mg^{-1}.min^{-1}) is the initial adsorption rate and β (mg.g^{-1}.min^{-1}) is the desorption coefficient.

The following equations were used to derive the thermodynamic parameters (H, S, and G):

$$\ln K_c = \frac{-\Delta H}{RT} + \frac{\Delta S}{R} \quad (6)$$

$$\Delta G = \Delta H - T\Delta S \quad (7)$$

$$\Delta G = -RT \ln K_c \quad (8)$$

Enthalpy, entropy, and Gibbs free energy changes are represented by the letters H, S, and G, respectively. T stands for temperature in Kelvin, and R is approximately (≈8.314 J K-1 mol^{-1}), the gas constant. The equilibrium values for retaining B.G. dye from the test aqueous solution onto the solid sorbent are determined by the equilibrium constant K_C. The values of K_C for retention of B are in the following equation:

$$\boldsymbol{k_c} = \frac{\boldsymbol{C_a}}{\boldsymbol{C_e}} \quad (9)$$

where Ce is the amount of B.G. dye adsorbed onto the solid phase per liter at equilibrium (mg L^{-1}), while Ca is the equilibrium concentration of B.G. dye in aqueous solution (mg L^{-1}).

RESULTS AND DISCUSSION

Characterization of PHBV/Ni-CuO bionanocomposites

The synthesized Ni-CuO nanoparticles – with Ni percentage of 10 mol% – were added to the PHBV neat polymer to form bionanocomposites with different percentages (1, 3, 5 and 10%), and will be referred to as PHBV/Ni-CuO$_{(x\%)}$ throughout the coming context, where x is the percentage of the added Ni-CuO nanofiller. In order to study the synthesized nanoparticles and

the new nanocomposites' characteristics, the samples were tested with FTIR, XRD, SEM and EDX.

The FTIR spectra of the bionanocomposites PHBV/Ni-CuO($_{x\%}$) and neat PHBV are shown in Figure 1. The characteristic peak of PHBV is the intense peak at 1720 cm^{-1} that corresponds to the ester carbonyl C=O stretching frequency, which also appears as an intense peak in all synthesized composites with various percentages. The peaks at 1379 cm^{-1} and 1453 cm^{-1} correspond to the amorphous part of the polymer.[46] The peaks at 2874 cm^{-1}, 2936 cm^{-1} and 2978 cm^{-1} refer to the different C-H stretching frequencies.[46] The intensities of the FTIR peaks for all percentages of nanoparticles in the composites have not changed significantly, which implies that there is a weak interaction between the nanofiller particles and the polymer chains, the most intense peak in the spectrum of Ni-CuO nanoparticles is the one at 1100 cm^{-1}, which also appears in an increasing intensity – as expected – within the spectra of the prepared composites as the percentage of the nanofiller increases. The FTIR spectrum of the Ni-CuO nanoparticles is very similar to previously reported findings for the same particles synthesized from the same source.[47]

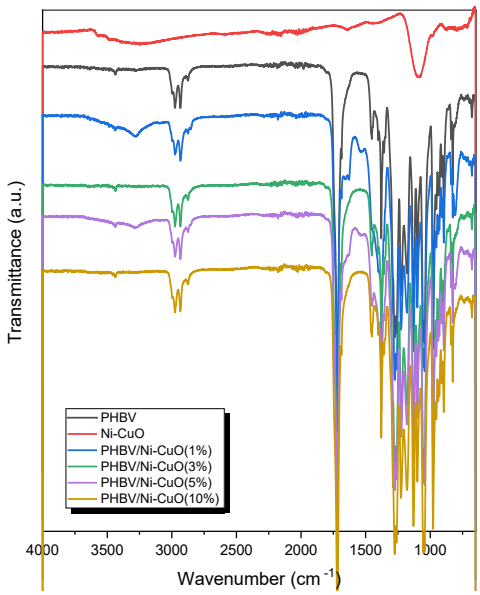

Figure 1: FTIR spectra of hybrid Ni-CuO, pure and PHBV/Ni-CuO$_{(1,3,5,10\%)}$ bionanocomposites

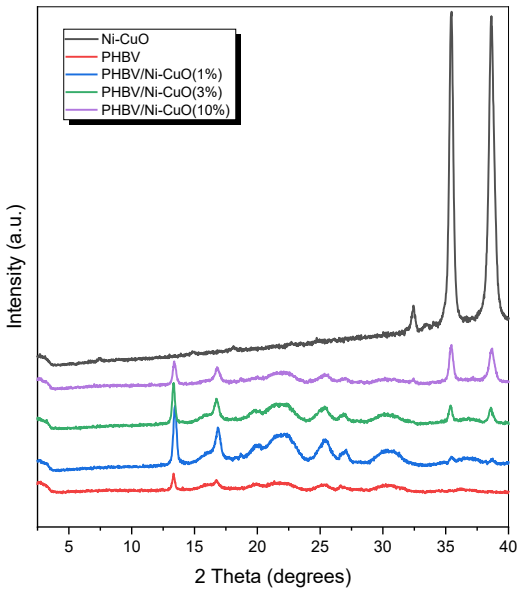

Figure 2: XRD spectra of hybrid Ni-CuO, pure and PHBV/Ni-CuO$_{(1,3,10\%)}$ bionanocomposites

The XRD spectrum of Ni-CuO (Fig. 2) shows characteristic peaks at 2θ = 32.44º, 35.43º and 38.63º, which are supposed to correspond to the planes in the monoclinic crystalline form of CuO (110), (002) and (111) respectively. A conclusion that can be made is that the monoclinic crystalline form of CuO has not been affected by Ni-doping, but still the overall crystallinity has been affected, as there was a considerable drop in the intensity of the peaks of Ni-CuO, compared to CuO (JCPDS card no 45-0937). These results are very similar to those of previously reported work, which showed XRD peaks of Ni-CuO at 33.11º, 35.84º and 38.58º.[47] The absence of nickel oxide diffraction peaks can indicate that the crystalline structure of CuO was not changed by Ni doping, but the slight shift in the diffraction angles towards slightly lower values indicated that Ni has been incorporated into the CuO lattice, this conclusion is justified by the close dimensions of the radii of both nuclei of Ni^{+2} (0.69 Aº) and Cu^{+2} (0.73 Aº). This finding is in harmony with the previously reported results for the same study.[47] The PHBV polymer exhibits the well-known characteristic peaks at 2θ values of 13.7°, 17.1°, 20.4°, 21.5°, 22.7°, 25.5°, 26.9°, 30.6°, which refer to the typically reported (020), (110), (021), (101), (111), (121), (040), (200) planes for orthorhombic PHBV, respectively.[47,48] The intense peaks as 13.7° and 17.1° are connected with the crystalline part of the polymer, while the broad peaks at 2θ =20º to 22º correspond to the amorphous phase in the PHBV.[45] For the purpose of studying the crystallization behavior of the nanocomposites compared to the neat PHBV, the investigated diffraction peaks' positions of the

planes (020), (110) and (040) have shown no significant changes in their positions, which implies that the formed nanocomposites are highly crystalline in nature. Also, as expected, the peaks at 2θ = 32.44º, 35.43º and 38.63º corresponding to the nanofiller are increasing in intensity with the increased filler percentage.

In addition, for further investigation, the changes in the thermal properties of PHBV pure polymer and its related bionanocomposites, samples of neat PHBV, Ni-CuO nanoparticles and their bionanocomposites PHBV/Ni-$CuO_{(1,5,10\%)}$ have been subjected to thermogravimetric analysis in the temperature region from RT to 800 °C, as shown in Figure 3. The thermograms show an initial small weight loss from RT up to 165 °C, which is attributed to the removal of water vapor and entrapped solvent.

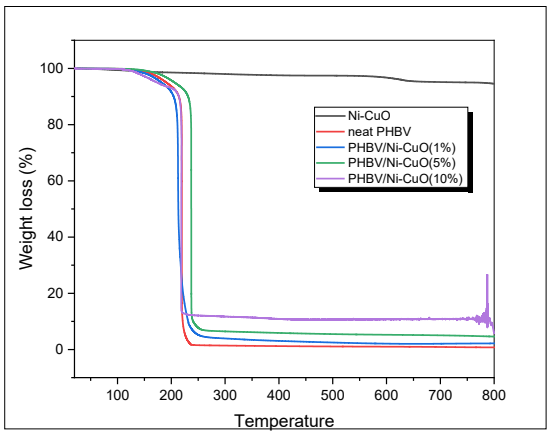

Figure 3: TGA thermograms of hybrid Ni-CuO, pure PHBV and PHBV/Ni-$CuO_{(1,5,10\%)}$ bionanocomposites

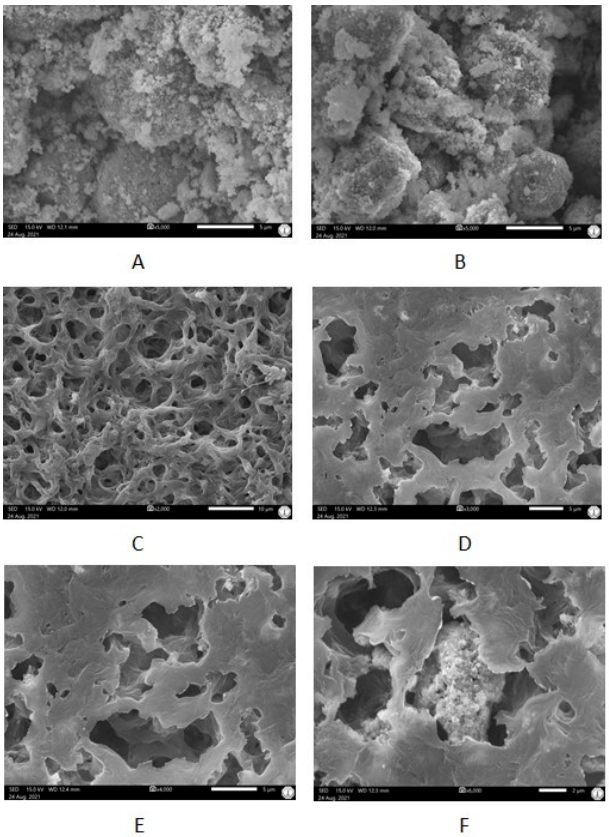

Figure 4: SEM micrographs: (A) Ni-CuO nanoparticles with 4k magnification; (B) Ni-CuO nanoparticles with 5k magnification; (C) PHBV/Ni-$CuO_{(1\%)}$, 2k magnification; (D) PHBV/Ni-$CuO_{(3\%)}$, 3k magnification; (E) PHBV/Ni-$CuO_{(3\%)}$, 4k magnification; (F) PHBV/Ni-$CuO_{(3\%)}$, 6k magnification

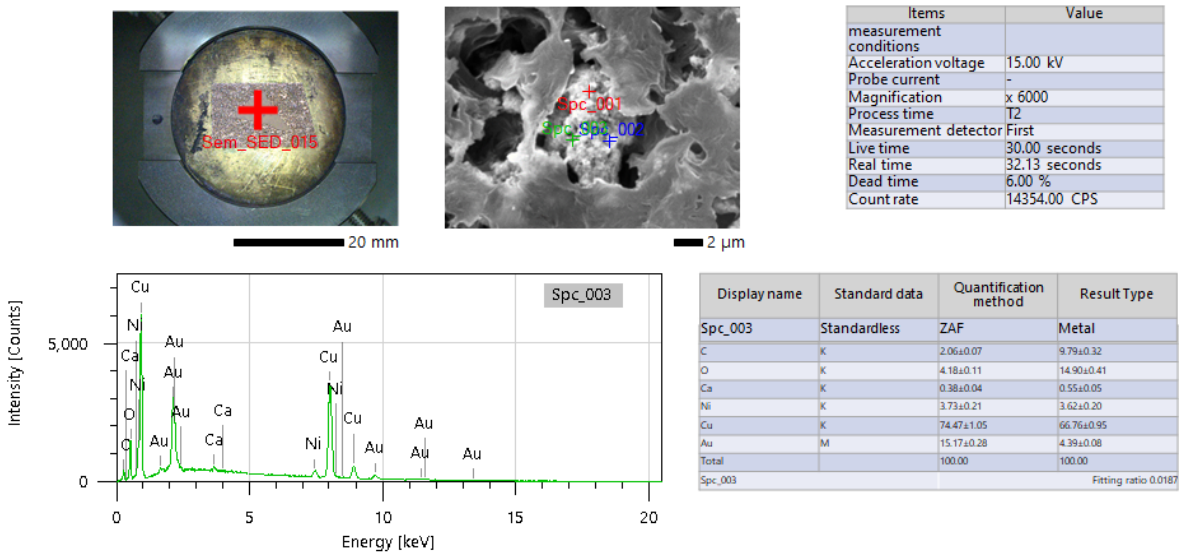

Figure 5: EDX analysis of highlighted point Spc 003 in SEM micrographs

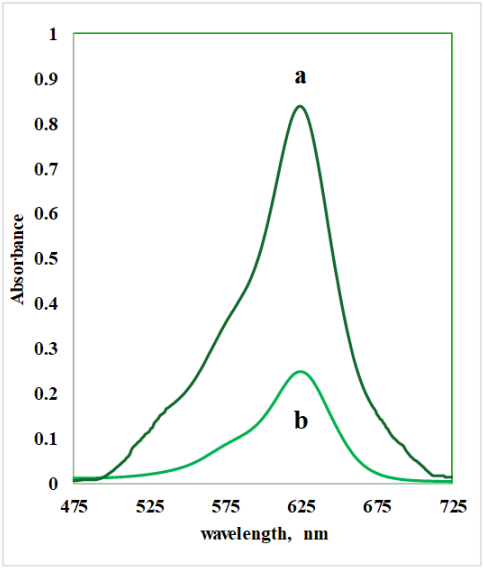

Figure 6: Absorbance spectra of B.G. dye in aqueous solution without nanocomposite solid phase added (a) and after 90 minutes shaking with the added solid phase nanocomposite (b)

The hybrid Ni-CuO filler shows a typical mixed metal oxides thermogram, as reported in the literature. The results indicated an enhancement in the thermal properties for all synthesized and analyzed bionanocomposites compared to the neat polymer.

All bionanocomposites PHBV/Ni-$CuO_{(1,5,10\%)}$ show a similar extremely fast pattern of decomposition. One step of decomposition has been observed for all samples to start at 210 °C and end at 245 °C. The degradation temperature is increased and the effect was more prominent in the case of the higher percentages till PHBV/Ni-$CuO_{(5\%)}$, then gradually decreased. These results are expected due to the expected higher thermal stability of the reinforced hybrid Ni-CuO fillers. The pure PHBV shows a complete weight loss % (almost completely decomposed without any residual products); while the other bionanocomposites display a gradual residue, which in agreement with the loading % of the hybrid Ni-CuO nanofiller.

The images of SEM for the Ni-CuO nanoparticles are shown in Figure 4 (A, B), they were similar to those reported before and confirmed the nanoparticles size ranging from 20-30 nm, as fine spheres that are forming different sizes of agglomerates, showing some fluffy structures.[47]

The existence of Ni and Cu was also confirmed by the EDX analysis of specific spots observed during SEM imaging, as illustrated in Figure 5. Also, images of the composites with different formulations are shown in Figure 4 (C-F); these composites' images show unevenly distributed agglomerates of the nanoparticles within the hollow and tubular network-shaped polymer chains. The Au peaks appearing in this figure are due to the gold coating used for SEM sample preparation, as shown in Figure 5.

Ni-CuO/PHBV$_{(3\%)}$ as solid phase for B.G. dye removal from aqueous solution samples

The aqueous solution of B.G. dye showed an absorption peak at 625±2 nm, however, this peak dramatically decreased after shaking in contact with the solid phase nanocomposites, as seen in Figure 6, and this result confirmed the efficiency of the solid phase nanocomposites for dye removal from aqueous solution.

Brilliant Green dye removal profile under different conditions

The solution pH is an important operating parameter that affects the efficiency of adsorption and recovery of both heavy metal ions and dyes. The adsorption efficiency (E) of the solid phase nanocomposite for the B.G. dyes at different pH was investigated after shaking for 90 min at room temperature. The photometric method was employed to determine the concentration of dye in the aqueous phase at equilibrium.[45] As shown in Figure 7, the solution pH has a considerable effect on the dye adsorption efficiency, the adsorption percentage, % E of B.G. by the nanocomposite has increased with increasing pH of the solution until pH = 6, and adsorption efficiency declines as the pH increases above 6. Data are shown in Figure 7. Hence, the pH = 6 was selected and considered as the optimum value for B.G. removal.

The effect of solid phase nanocomposite mass on the dye adsorption percentage was investigated for B.G. at a concentration of 5 mg/L, as seen in Figure 8. The results showed that, as the nanocomposite amount increased from 10 mg to 70 mg per 25 mL of water sample, the percentage of the removed dye increased from 45.6% to 97.7%. This increase in removal efficiency was attributed to the larger number of available active sites for the adsorption. Hence, in this research work, 30 mg of the nanocomposite per 25 mL of water sample, which gave 73.7% dye removal, was used as optimum amount to study the effect of other operating parameters on the dye adsorption and its removal from water samples.

The time of contact between the adsorbent and the adsorbate is also another considerable factor/operating parameter that affects the efficiency of pollutants removal by adsorption. This effect was studied on the dye removal by the nanocomposite and the results are shown in Figure 9. The results have shown that, as the contact time increases, the adsorption efficiency does as well. This effect was prominent during the first 60 min, where most of the dye was adsorbed. The dye removal percentage reached an equilibrium in 90 min, and this suggests that the adsorption of dye on the nanocomposite is a two-step process, the first one, being the fastest, is the transfer of dye species from the aqueous phase to the nanocomposite external surfaces. Then, the second and a slower step is the diffusion of dye species between the nanocomposite interlayers.

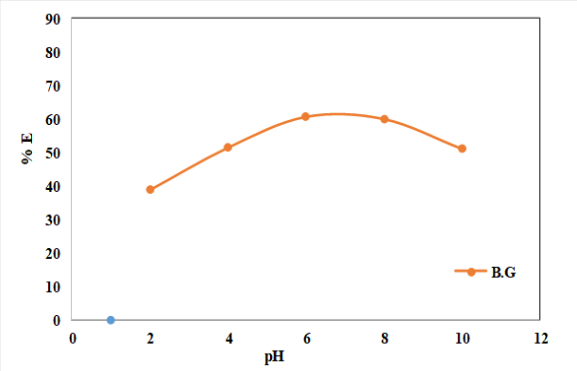

Figure 7: Effect of pH on the adsorption percentage of B.G. dye (5 mgL^{-1}) from aqueous solutions onto (0.03 g per 25 mL of water sample) nanocomposite with 90 min shaking time at 20 °C

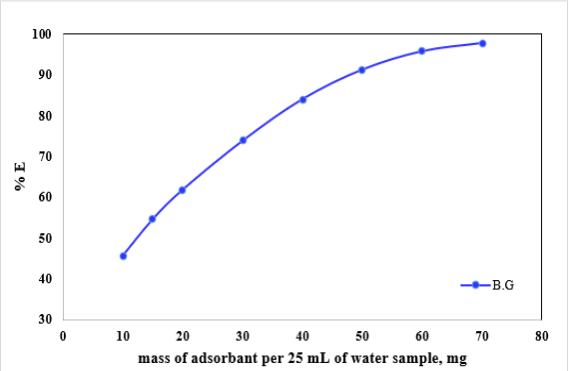

Figure 8: Effect of nanocomposite mass per 25 mL of sample on the percentage of B.G. (5 mgL^{-1}) dye adsorption at pH = 6 at 20 °C and shaking time of 90 min

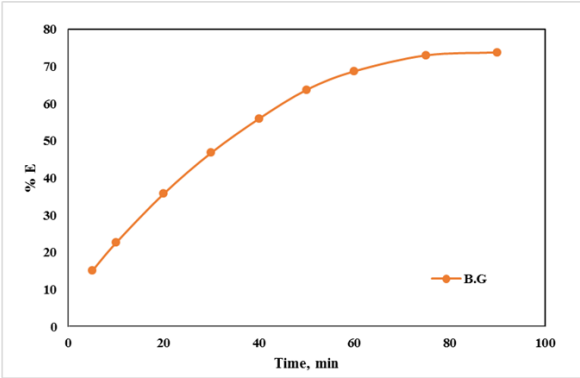

Figure 9: Shaking time effect on the adsorption percentage of B.G. dye (5 mgL^{-1}) at pH = 6 onto the nanocomposite at 20 °C

In addition, the temperature of the solution also affects the adsorption process, so it was studied by using four different temperatures: 283 K, 293 K, 308 K and 323 K at constant shaking time. The results have shown that there was a significant increase in the adsorption efficiency (B.G. (5 mgL^{-1}) dye adsorption at pH = 6 at 20 °C and shaking time of 90 min), when the temperature of the solution was raised from 283 K to 323 K, as shown in Figure 10. These results indicate an endothermic process of the adsorption.

The ionic strength of the solution is also an important operating parameter that affects the adsorption process due to electrostatic interactions between the solid phase surfaces and the dye species. The effect of ionic strength on B.G. (5 mgL^{-1}) dye adsorption at pH = 6 at 20 °C and shaking time (90 min) onto the nanocomposite solid phase was investigated via changing the solution ionic strength with different KNO_3 concentrations of 0.025, 0.05, 0.075 and 0.1 mol/L, as shown in Figure 11. The results showed that increasing the ionic strength in the aqueous solution has resulted in a slight decrease in the adsorption efficiency. This can be attributed to the fact that the presence of the additional cations and anions would decrease the dye species interaction with the surface of the adsorbent, as more charges are accumulated adjacent to the adsorbent surface.[49]

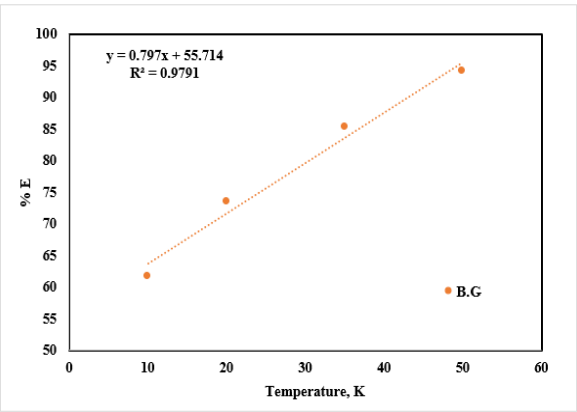

Figure 10: Effect of temperature on the adsorption percentage of dye species B.G. (5 mgL^{-1}) at pH = 6 from aqueous solutions onto nanocomposite at 283 K, 293 K, 308 K and 323 K and shaking time of 90 min

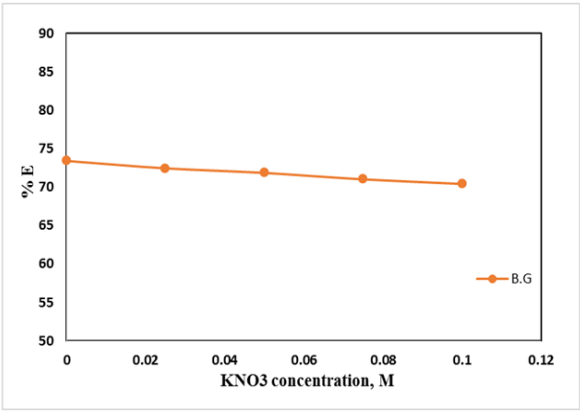

Figure 11: Effect of KNO_3 concentration on the adsorption percentage of dye species B.G. from aqueous solutions onto the nanocomposite at 20 °C temperature

Adsorption kinetic study of Brilliant Green onto Ni-CuO/PHBV$_{(3\%)}$ solid phase adsorbent

The study examines the dynamics of B.G. dye sorption onto the Ni-CuO/PHBV$_{(3\%)}$ solid phase. Understanding this sorption process is crucial for understanding the underlying mechanics. It mostly depends on intraparticle diffusion and film diffusion, with the former two determining the overall transport rate. The conclusion is supported by calculating the half-life time ($t_{1/2}$) for B.G. dye sorption onto Ni-CuO/PHBV$_{(3\%)}$, as well as looking at the impact of shaking time. According

to calculations, the $t_{1/2}$ value for B.G. dye is 1.6 ± 0.05 minutes, which is in line with earlier findings.[50] This confirms that the faster intraparticle diffusion determines the total rate of transport, with sorption kinetics dependent on both film and intraparticle diffusion, with the faster one dictating the overall rate of transport.

The Weber-Morris model is utilized in the study to conduct additional research on the sorption process (Eq. 1, previously mentioned). The dynamics of how contaminants, including dye species, are removed from aqueous solutions by solid sorbents is essential, because it sheds light on the reaction pathways and the mechanisms underlying the sorption processes. Film diffusion and intraparticle diffusion are both required for dye species to remain on the solid phase Ni-CuO/PHBV$_{(3\%)}$, and whichever one is more rapid will determine the rate of transport as a whole.

Five main kinetic models were applied to explain the adsorption process.[51-56] In Figure 12, the plot of qt over time was represented. R_d was determined to be the equivalent of 0.37 mg g^{-1} for B.G. dye, employing the distinct slope of Weber-Morris plots (Fig. 12) and a correlation coefficient of $R^2 = 0.981$.

This model links the sorbed B.G. dye concentration (qt) at various times to the rate constant of intraparticle transport (R_d).[51] With a high correlation coefficient (R^2 = 0.981), the calculated R_d value for B.G. dye is determined to be 0.37 mg g^{-1}.

The Freundlich equation is also used to generate a fractional power function kinetic model, which is used to explain the adsorption process. The fractional power function equation is applied to the experimental data of the adsorption process, as illustrated in Figure 13. The experimental data and this model agree well, with the correlation coefficient (R^2) for B.G. dye coming in at 0.993. Given the specific values of a and b in Table 1, it can be concluded that the adsorption of dye species by Ni-CuO/PHBV$_{(3\%)}$ is adequately described by the fractional power function kinetic model.

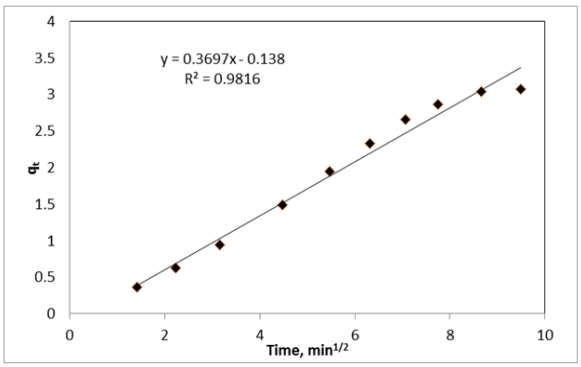

Figure 12: Weber–Morris plot of the sorbed dye B.G. from aqueous solutions onto Ni-CuO/PHBV$_{(3\%)}$ versus square root of time. Conditions are mentioned in the experimental section

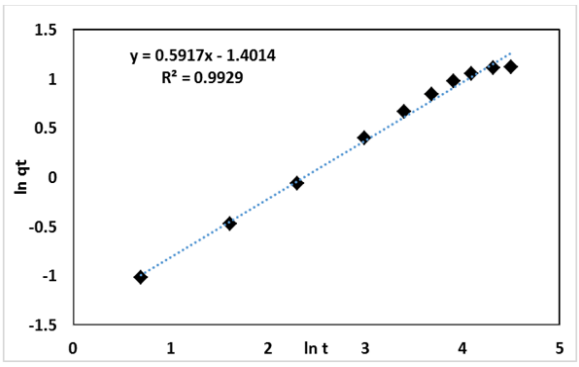

Figure 13: Fractional power model plots of dye B.G. from aqueous solutions onto Ni-CuO/PHBV$_{(3\%)}$. Conditions are mentioned in the experimental section

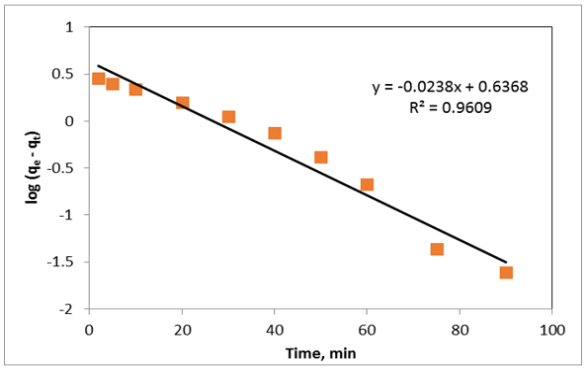

Figure 14: Lagergren plot of dye B.G. uptake onto Ni-CuO/PHBV$_{(3\%)}$ versus time. Conditions are mentioned in the experimental section

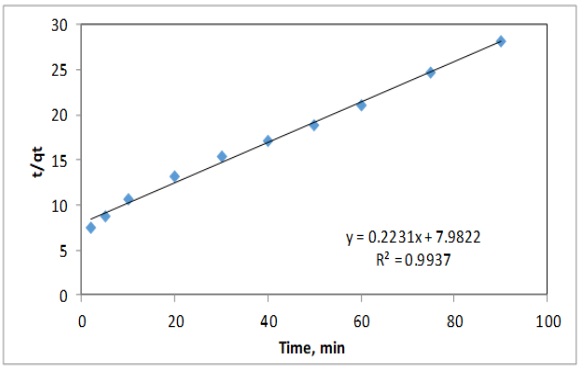

Figure 15: Pseudo-second order plot of dye B.G. uptake onto Ni-CuO/PHBV$_{(3\%)}$ versus time. Conditions are mentioned in the experimental section

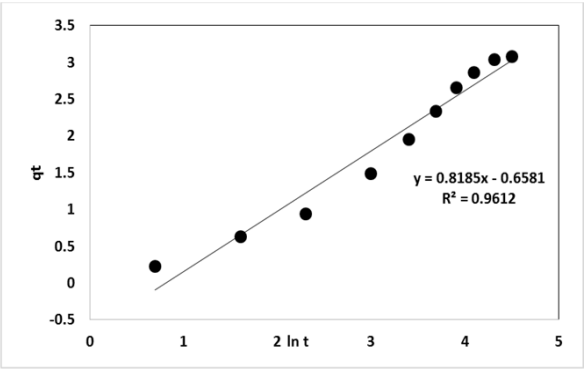

Figure 16: Elovich model plot for dye B.G. uptake onto Ni-CuO/PHBV$_{(3\%)}$ versus time. Conditions are mentioned in the experimental section

The Lagergren (the pseudo-first-order kinetic) model was also investigated. The computed values of K_{Lager} and q_e were found to be equal to 0.055 min^{-1} and 4.34 mg/g for B.G. dye, with correlation coefficient R^2 = 0.961, although all of this data is inconclusive.

The pseudo-second order equation was further clarified as shown in Figure 15. The slope and intercept for B.G. dye was used to compute the second-order rate constant (k_2) and equilibrium capacity (q_e) for dye species. These values were found to be 6 x 10^{-3} g (mg.min)$^{-1}$ and 4.55 mg/g, respectively, with an excellent correlation (R^2 = 0.994). The findings demonstrate that all experiments' outcomes are in good agreement with each other and with the values of the pseudo-second order rate constant, k_2, which is frequently affected by the variables being studied, such as initial metal concentration, solution pH, and temperature.

The Elovich model, which is a common method of expressing the rate equation based on adsorption capacity was illustrated in Figure 16. The plot of q_t versus ln t was linear (Fig. 16). The Elovich parameters α and β computed from the intercepts and the slopes in Figure 16 for the dye species were found equal with 2.73 g.mg^{-1}.min^{-1} and 0.82 mg.g^{-1}.min^{-1}, respectively with R^2 = 0.961, for B.G. dye adsorbed onto Ni-CuO/PHBV$_{(3\%)}$.

A comparative illustration for the variable kinetic model's parameters for the adsorption of B.G. dye by Ni-CuO/PHBV$_{(3\%)}$ sorbent is displayed in Table 1.

Table 1
Parameters of different kinetic models for the adsorption of B.G. dye on Ni-CuO/PHBV$_{(3\%)}$, at 293 K

Weber–Morris model				
B.G.		R_d		R^2
		0.37		0.981
Fractional power function kinetic (Freundlich) model				
B.G.	a	b	ab	R^2
	0.247	0.592	0.146	0.992
Pseudo-first-order kinetic(lagregen) model				
B.G.	$q_{e,\,exp}$ (mg/g)	$q_{e,\,calc}$ (mg/g)	k_1	R^2
	3.06	4.34	0.055	0.961
Pseudo-second-order kinetic model				
B.G.	$q_{e,\,exp}$ (mg/g)	$q_{e,\,calc}$ (mg/g)	k_2	R^2
	3.06	4.55	6 x 10^{-3}	0.994
Elovich kinetic model				
B.G.	α (g/mg min)	β (mg/g min)		R^2
	2.73	0.819		0.961

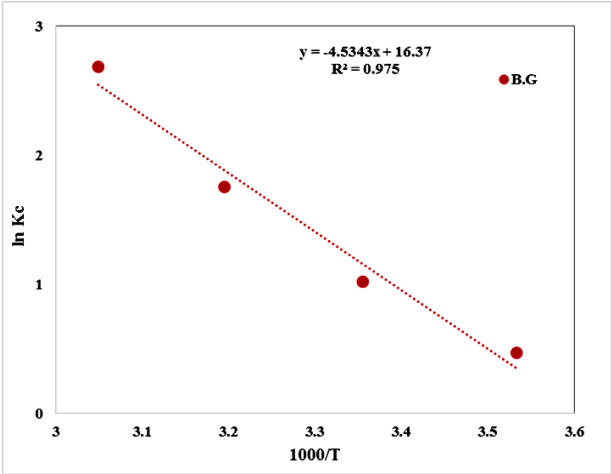

Figure 17: Plot of ln K_C of B.G. dye sorption from aqueous media onto Ni-CuO/PHBV$_{(3\%)}$ versus 1000/T

Thermodynamic characteristics of B.G. dye retention onto Ni-CuO/PHBV$_{(3\%)}$

In this study, the sorption of B.G. dye onto Ni-CuO/PHBV$_{(3\%)}$ solid phase was examined throughout a temperature range of 283–323 K. The analysis of dye species retention on Ni-CuO/PHBV$_{(3\%)}$ was the primary objective. For B.G. dye retention onto Ni-CuO/PHBV$_{(3\%)}$ solid phase, the plot of ln K_C vs 1000/T was linear (Fig. 10) over the temperature range (283-323 K). The endothermic character of the B.G. dye's retention process on the utilized sorbents is shown by the increase in temperature of the equilibrium constant. According to the slope and intercept of the linear plot of ln KC vs 1000/T (Fig. 17), the numerical values of ΔH, S, and G for B.G. dye species retention were calculated to be 37.66 ± 0.3 kJ mol^{-1}, 136.1 ± 0.4 J mol^{-1} K^{-1} and -2.21 ± 0.1 kJ mol^{-1} (at 293 K), respectively.

The ΔH value demonstrates the degree of endothermicity in the adsorption process, and also reflects the disparity in bond strengths between the sorbent and the analyte. The increase in the degree of freedom at the solid-liquid interface, that is often observed in B.G. dye species binding due to the release of water molecules from the hydration sphere during the adsorption processes, was suggested by the positive value of S for the solid phase Ni-CuO/PHBV$_{(3\%)}$. The produced solid phase's negative ΔG value at 293 K indicates dye species retention on Ni-CuO/PHBV$_{(3\%)}$ is the result of physical sorption rather than chemical sorption.

The pseudo-second-order kinetic model is the most appropriate kinetic model to describe the adsorption of dye species by Ni-CuO/PHBV$_{(3\%)}$ from an aqueous solution, according to the results from the kinetic models used to fit the experimental data on the adsorption of B.G. dye species. These models included the fractional power function, Lagergren pseudo-first-order, pseudo-second-order, and the Elovich models.

Testing Ni-CuO/PHBV$_{(3\%)}$ nanocomposite for B.G. dye removal in natural water samples

Three samples of natural water were collected to test the efficiency of the Ni-CuO/PHBV$_{(3\%)}$ nanocomposite in removing B.G. dye: tap water from Saudi Arabia, wastewater from King Abdulaziz University, and seawater from the Red Sea shore. B.G. concentrations initially were below detection limits. 70 mg of nanocomposite was introduced into each 25 mL of the water samples under investigation. The pH was subsequently adjusted to 6, shacking time 90 minutes at 293 K and the samples were then contaminated with 5 mg L^{-1} of B.G. The percentage removal of B.G. dye is shown in Figure 18. Subsequently, the nanocomposites were collected, purified, and dehydrated prior to their application in the elimination of B.G dye. Four consecutive rounds of nanocomposite use were successfully performed. Figure 18 shows that the E% was 96, 92 and 90% for tap water, wastewater and sea water samples. After four cycles, the outcomes were almost equal to the initial percent of removal for each kind of water. When compared to the other two water sources, the E% of the tap water is the highest. It is possible that this is because of the interference that might take place involving other ions that are present in both water sources.

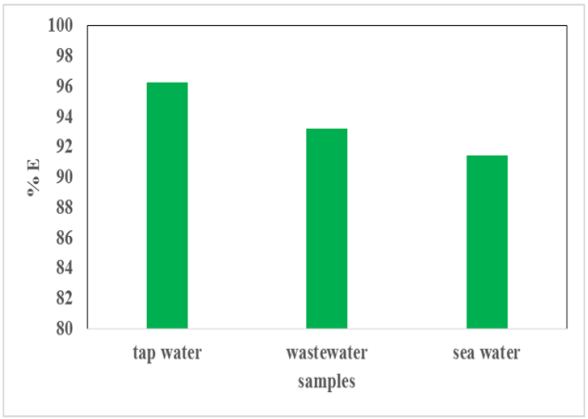

Figure 18: Removal percentages of B.G. dye from different natural water samples by using the Ni-CuO/PHBV$_{(3\%)}$ nanocomposite solid phase (experimental conditions: 25 mL solution, pH = 6, B.G. concentration 5 mg L^{-1} and 70 mg of nanocomposite, shaking time = 90 min, Temp. = 293 K)

CONCLUSION

Biosynthesized PHBV polymer and Ni-CuO nanoparticles with a 10 mol% Ni content were successfully combined to produce bionanocomposites with 1%, 3%, 5%, and 10% loading ratios, denoted in this work as PHBV/Ni-CuO. FTIR, TGA, XRD, SEM, and EDX were utilized to confirm the chemical structures of the fabricated bionanocomposites and to study their essential characteristics. Then, under different testing options, they were assessed as solid phase adsorbents for the elimination of Brilliant Green dye from different water sources. Based on the results, these nanocomposites are highly efficient and promising materials for eliminating dyes in environmental water treatments.

ACKNOWLEDGMENTS: The Deanship of Scientific Research (DSR), at King Abdulaziz University (KAU), Jeddah, Saudi Arabia, has funded this project, under grant no. KEP-PhD: 60-130-1443.

REFERENCES

[1] E. Bugnicourt, P. Cinelli, A. Lazzeri and V. Alvarez, *eXPRESS Polym. Lett.*, **8**, 791 (2014), https://doi.org/10.3144/expresspolymlett.2014.82

[2] K. Zhao, Y. Deng, J. C. Chen and G. Q. Chen, *Biomaterials*, **24**, 1041 (2003), https://doi.org/10.1016/s0142-9612(02)00426-x

[3] S. Modi, K. Koelling and Y. Vodovotz, *Eur. Polym. J.*, **47**, 179 (2011), https://doi.org/10.1016/j.eurpolymj.2010.11.010

[4] X. Wang, Z. Chen, X. Chen, J. Pan and K. Xu, *J. Appl. Polym. Sci.*, **117**, 838 (2010), https://doi.org/10.1002/app.31215

[5] H. J. Endres and A. Siebert-Raths, "Engineering Biopolymers Markets, Manufacturing, Properties, and Applications", Munich, Carl Hanser Verlag, 2011, https://doi.org/10.3139/9783446430020

[6] M. Larsson, O. Markbo and P. Jannasch, *RSC Adv.*, **6**, 44354 (2016), https://doi.org/10.1039/C6RA06282B

[7] Y. X. Weng, Y. Wang, X. L. Wang and Y. Z. Wang, *Polym. Test.*, **29**, 579 (2010), https://doi.org/10.1016/j.polymertesting.2010.04.002

[8] M. Avella, E. Martuscelli and M. Raimo, *J. Mater. Sci.*, **35**, 523 (2000), https://doi.org/10.1023/A:1004740522751

[9] P. B. Malafaya, G. A. Silva and R. L. Reis, *Adv. Drug Deliv. Rev.*, **59**, 207 (2007), https://doi.org/10.1016/j.addr.2007.03.012

[10] C. S. Ha and W. J. Cho, *Prog. Polym. Sci.*, **27**, 759 (2002), https://doi.org/10.1016/S0079-6700(01)00050-8

[11] B. S. Thorat Gadgil, N. Killi and G. V. N. Rathna, *Medchemcomm*, **8**, 1774 (2017), https://doi.org/10.1039/C7MD00252A

[12] Z. Li, J. Yang and X. J. Loh *NPG Asia Mater.*, **8**, e265 (2016), https://doi.org/10.1038/am.2016.48

[13] M. I. Ibrahim, D. Alsafadi, K. A. Alamry and M. A. Hussein, *J. Polym. Environ.*, **2021**, 1010 (2021), https://doi.org/10.1007/s10924-020-01946-x

[14] J. Lim, M. You, J. Li and Z. Li, *Mater. Sci. Eng. C*, **79**, 917 (2017), https://doi.org/10.1016/j.msec.2017.05.132

[15] R. Dwivedi, R. Pandey, S. Kumar and D. Mehrotra, *J. Oral Biol. Craniofac. Res.*, **10**, 389 (2020), https://doi.org/10.1016/j.jobcr.2019.10.004

[16] J. Zhang, E. I. Shishatskaya, T. G. Volova, L. F. da Silva and G. Q. Chen, *Mater. Sci. Eng. C*, **86**, 144 (2018), https://doi.org/10.1016/j.msec.2017.12.035

[17] J. L. C. Mayorga, M. J. F. Rovira, L. C. Mas, G. S. Moragas and J. M. L. Cabello, *J. Appl. Polym. Sci.*, **135**, 45673 (2017), https://doi.org/10.1002/app.45673

[18] K. Mazur, R. Singh, R. P. Friedrich, H. Genç, H. Unterweger *et al*., *Macromol. Mater. Eng*., **305**, 2000244 (2020), https://doi.org/10.1002/mame.202000244
[19] N. Salahuddin, M. Gaber, M. Mousa and M. A. Abdelwahab, *RSC Adv*., **10**, 34046 (2020), https://doi.org/10.1039/D0RA04784H
[20] A. H. Mahvi, M. Malakootian and M. R. Heidari, *J. Water Chem. Technol*., **33**, 377 (2011), https://doi.org/10.3103/S1063455X11060051
[21] M. Malakootian, N. Radhakrishna, M. P. Mazandarany and H. Hossaini, *Desalin. Water Treat*., **51**, 4478 (2013), https://doi.org/10.1080/19443994.2013.769668
[22] X. Zheng, Z. Zhang, D. Yu, X. Chen, R. Cheng *et al*., *Resour. Conserv. Recycl*., **105**, 1 (2015), https://doi.org/10.1016/j.resconrec.2015.09.012
[23] V. Singh, A. Tiwari and M. Das, *Fuel*, **173,** 90 (2016), https://doi.org/10.1016/j.fuel.2016.01.031
[24] S. Natarajan, H. C. Bajaj and R. J. Tayade, *J. Environ. Sci*., **65**, 201 (2018), https://doi.org/10.1016/j.jes.2017.03.011
[25] E. A. Dil, M. Ghaedi, A. M. Ghaedi, A. Asfaram, A. Goudarzi *et al*., *J. Ind. Eng. Chem*., **34**, 186 (2016), https://doi.org/10.1016/j.jiec.2015.11.010
[26] A. Ayach, S. Fakhi, Z. Faiz, A. Bouih, O. Ait Malek *et al*., *Chem. Int*., **3**, 442 (2017)
[27] M. Abbas, M. Adil, S. Ehtisham-ul-Haque, B. Munir, M. Yameen *et al*., *Sci. Total Environ*., **626**, 1295 (2018), https://doi.org/10.1016/j.scitotenv.2018.01.066
[28] S. de Gisi, G. Lofrano, M. Grassi and M. Notarnicola, *Sustain. Mater. Technol*., **9**, 10 (2016), https://doi.org/10.1016/j.susmat.2016.06.002
[29] Y. Zhang, B. Wu and H. Xu, *NanoImpact*, **3-4**, 22 (2016), https://doi.org/10.1016/j.impact.2016.09.004
[30] M. Iqbal, M. Abbas and A. Nazir, *Chem. Int*., **5**, 1 (2019), https://doi.org/10.5281/zenodo.1475399
[31] M. Malakootian, A. Nasiri, A. Asadipour and E. Kargar, *Process Saf. Environ. Prot*., **129**, 138 (2019), https://doi.org/10.1016/j.psep.2019.06.022
[32] R. Saravanan, V. K. Gupta, V. Narayanan and A. Stephen, *J. Taiwan Inst. Chem. Eng*., **45**, 1910 (2014), https://doi.org/10.1016/j.jtice.2013.12.021
[33] A. Kausar, M. Iqbal and A. Javed, *J. Mol. Liq*., **256**, 395 (2018), https://doi.org/10.1016/j.molliq.2018.02.034
[34] V. Katheresan, J. Kansedo and S. Y. Lau, *J. Environ. Chem. Eng*., **6**, 4676 (2018), https://doi.org/10.1016/j.jece.2018.06.060
[35] A. F. S. Costa, C. D. C. Albuquerque, A. A. Salgueiro and L. A. Sarubbo, *Process Saf. Environ. Prot*., **118**, 203 (2018), https://doi.org/10.1016/j.psep.2018.03.001
[36] B. Bharathiraja, I. A. E. Selvakumari, J. Iyyappan and S. Varjani, *Curr. Opin. Environ. Sci. Health*, **12**, 6 (2019), https://doi.org/10.1016/j.coesh.2019.07.004
[37] A. Saravanan, R. Jayasree and R. V. Hemavathy, *J. Environ. Chem. Eng*., **7**, 103052 (2019), https://doi.org/10.1016/j.jece.2019.103052
[38] T. R. Sahoo and B. Prelot, *Micro Nano Technol*., **2020**, 161 (2020), https://doi.org/10.1016/B978-0-12-818489-9.00007-4
[39] M. A. El-Ghobashy, I. A. Salem, W. M. El-Dahrawy and M. A. Salem, *J. Mol. Struct*., **1272**, 134118 (2023), https://doi.org/10.1016/j.molstruc.2022.134118
[40] M. El-Sakhawy, A. Salama, A. K. El-Ziaty and H. Hassan, *Cellulose Chem. Technol*., **54**, 601 (2020), https://doi.org/10.35812/cellulosechemtechnol.2020.54.60
[41] S. Moosavi, S. Gan and S. Zakaria, *Cellulose Chem. Technol*., **53**, 815 (2019), https://doi.org/10.35812/CelluloseChemTechnol.2019.53.80
[42] Rajapaksha, R. Orrell-Trigg, Y. B. Truong, D. Cozzolino, V. Truong *et al*., *Environ. Sci. Adv*., **1**, 456 (2022), https://doi.org/10.1039/D2VA00059H
[43] H. Khawaja, E. Zahir, M. A. Asghar and M. A. Asghar, *Int. J. Biol. Macromol*., **167**, 23 (2021), https://doi.org/10.1016/j.ijbiomac.2020.11.137
[44] D. Alsafadi, M. I. Ibrahim, K. A. Alamry, M. A. Hussein and A. Mansour, *Sci. Total Environ*., **737**, 139716 (2020), https://doi.org/10.1016/j.scitotenv.2020.139716
[45] Z. Marczenko, "Separation and Spectrophotometric Determination of Elements", 2nd ed., John Wiley and Sons, 1986
[46] R. Naphade and J. Jog, *Fibers Polym*., **13**, 692 (2012), https://doi.org/10.1007/s12221-012-0692-9
[47] L. M. Dwivedi, N. Shukla, K. Baranwal, S. Gupta, S. Siddique *et al*., *J. Cluster Sci*., **32**, 209 (2021), https://doi.org/10.1007/s10876-020-01779-7
[48] S. Vidhate, L. Innocentini-Mei and N. A. D'Souza, *Polym. Eng. Sci*., **10**, 1357 (2012), https://doi.org/10.1002/pen.23084
[49] S. A. Dastgheib and D. A. Rockstraw, *Carbon*, **40**, 1853 (2002), https://doi.org/10.1016/S0008-6223(02)00036-2
[50] H. M. Al-Saidi, M. A. Abdel-Fadeel, A. Z. El-Sonbati and A. A. El-Bindary, *J. Mol. Liq*., **216**, 693 (2016), https://doi.org/10.1016/j.molliq.2016.01.086
[51] W. J. Weber, J. C. Morris and J. Sanit, *Eng. Div. Am. Soc. Civ. Eng*., **89**, 31 (1963)
[52] R. C. Dalal, *Commun. Soil Sci. Plant Anal*., **5**, 531 (1974), https://doi.org/10.1080/00103627409366531
[53] A. K. Bhattacharya and C. Venkobachar, *J. Environ. Eng*., **110**, 1 (1984), https://doi.org/10.1061/(ASCE)0733-9372(1984)110:1(110)

[54] H. M. Al-Saidi, M. A. Abdel-Fadeel and S. S. Alharthi, *J. Saudi Chem. Soc.*, **25**, 101301 (2021), https://doi.org/10.1016/j.jscs.2021.101301
[55] R. H. Althomali, K. A. Alamry, M. A. Hussein, A. Khan, S. S. Al-Juaid *et al.*, *Int. J. Environ. Analyt. Chem.*, **102**, 3673 (2022), https://doi.org/10.1080/03067319.2020.1772772
[56] M. A. Abdel-Fadeel, N. S. Aljohani, S. R. Al-Mhyawi, R. F. Halawani, E. H. Aljuhani *et al.*, *J. Saudi Chem. Soc.*, **26**, 101475 (2022), https://doi.org/10.1016/j.jscs.2022.101475